

Preparation of Void-less Topographic Wetness Index for Hydrological Analysis using Digital Elevation Model

Sailesh Samanta

GIS Section, Department of Surveying and Land Studies, The Papua New Guinea University of Technology, Private mail Bag, Lae, Morobe, Papua New Guinea

rsgis.sailesh@gmail.com

Received: 29 June 2023 | Accepted: 19 October, 2023

Abstract

Geographic information system (GIS) is an important tool to generate different types of information from digital elevation model (DEM) within a watershed region, where topographical and hydrological characteristics are very important. Topographic wetness index (TWI) is one of the essential parameters in topographical and hydrological modeling, which can be developed from DEM. Estimating the amount of soil moisture is directly correlated with TWI and amount of rainfall. There are several ways to calculate TWI, which uses DEM in different spatial resolution (cell size), different types of slopes, flow direction, flow accumulation, soil properties and rainfall distribution. In this research, TWI was calculated based on six topographic parameters generated from DEM of 30m spatial resolution. They are slope in degree, radian of slope, tan slope, flow direction, flow accumulation and scaled flow accumulation. The result shows that the slope factor has a greater correlation with an R-square value of 0.38. This type of void-less TWI data is most important for topographic and hydrologic modeling in any watershed region.

Keywords: *Digital Elevation Model, Geographical Information System, Markham River Basin, Remote Sensing, Topographic Wetness Index*

1. Introduction

Soil moisture is one of the important variables controlling hydrological processes in a watershed region (Buchanan et al., 2014). Topographic wetness indicates the moisture content within the soil, has been widely integrated into numerous popular hydrologic models (Reaney et al., 2011; Samanta et al., 2018). Hydrological models can predict runoff characteristics, runoff rate and pattern over the earth surface within a river basin. Shuttle radar topographic mission (SRTM) and advanced space borne thermal emission and reflection radiometer (ASTER) are providing enhance void less digital elevation data with a medium to higher resolution. Digital elevation models (DEM) are commonly used for the land surface characterization and morphometric analysis in a watershed or river basin area (Yang et al., 2011). Widely availability of DEM data contributed detailed and perfect representation of earth surface topography (Buchanan et al., 2014). As a result, recent hydrological modeling is becoming faster and more accurate than earlier (Brookfield et al., 2023). Hydrological and topographical parameters derived from the DEM have been used as significant input parameters in climate modeling, hydrological modeling, land suitability modeling, landslide modeling, surface runoff and flood modeling

(Chowdhury, 2023) etc. Elevation, absolute relief, relative relief, dissection index, drainage density, ruggedness index, Slope, aspect, distance to stream, topographic wetness index (TWI) etc. are the few DEM based topographical, morphological and hydrological factor, which are the best choice by researchers around the world (Sorensen et al., 2006; Wang and Liu, 2006; Sujen and Kaya, 2012). These factors become more useful because of easy availability of open source DEM data, which can be processed through GIS software. TWI is one of the widely used and important parameters in hydrological analysis. The derivation of this TWI was initially introduced by Beven and Kirby (1979). TWI was integrated successfully into numbers of popular hydrologic models, like Topography-based hydrological model (TOPMODEL) (Beven and Kirby, 1979); Variable Source Loading Function (VSLF) (Schneiderman et al., 2007); Soil and water assessment tool variable source area (SWAT-VSA) Easton et al., 2008) etc.

Advancement of Remote Sensing, GIS and the availability of the high-resolution DEM data has helped to determine details and realistic presentation of topography. In the recent past, a number of researchers used 90 m DEM to determine TWI (Hojati and Mokarram, 2016; Koriche and Rientjes, 2016; Das, 2028). The primary objective of the study focused on the preparation of void less Topographic Wetness Index (TWI) datasets from DEM data. The spatial resolution 30m DEM and using ArcGIS v10.5 (ArcMap) software was used to fulfill the study objective. The detailed methodology is presented in this paper which is very much helpful in hydrological modeling and hazard modeling.

2. Materials and Methods

The Markham River starts from the Finisterre range and flow about 180km to empty into the Huon Gulf at Lae (Figure-1). The Markham watershed is dominated by mountain range, high up and down slope and primary forest. Major parts of Morobe province (94%) are situated within the Markham watershed. The entire watershed area is considered for this study.

2.1 Materials used

The Advanced Space borne Thermal Emission and Reflection Radiometer (ASTER) provide high resolution (30-meter spatial resolution) Global Digital Elevation Model (GDEM) (Abrams, 2000; Abrams et al., 2015). This elevation data covers almost 99% of the land area between 80° N to 80°S. The global digital elevation model version 2 (GDEM 2) was released in year 2011 in a degree tile footprint (Hu et al., 2017). The data sets for entire Papua New Guinea (PNG) were purchase from Intermap Technologies, Australia. Total number of tiles was 110, which were converted from Band Interleaved by Line (BIL) to Floating Point (FLT) using ArcGIS v10.1 and merged using ERDAS Imagine v-10.0 software. The mosaic data sets were re-projected to Universal Traverse Mercator (UTM) projection system.

2.2 Methods

The topographic wetness index (TWI) model (Equation 1) was initially developed by Beven and Kirkby in 1979. The same model was used to construct TWI parameters, which is mandatory input parameters in hydrological modeling (Grabs et al., 2009; Pourali et al., 2016; Chowdhury, 2023).

$$TWI = \ln \frac{\alpha}{\tan \beta} \quad (\text{eq. 1})$$

Where, α is the local upslope area draining through a certain point per unit contour length and $\tan \beta$ is the local slope in radian.

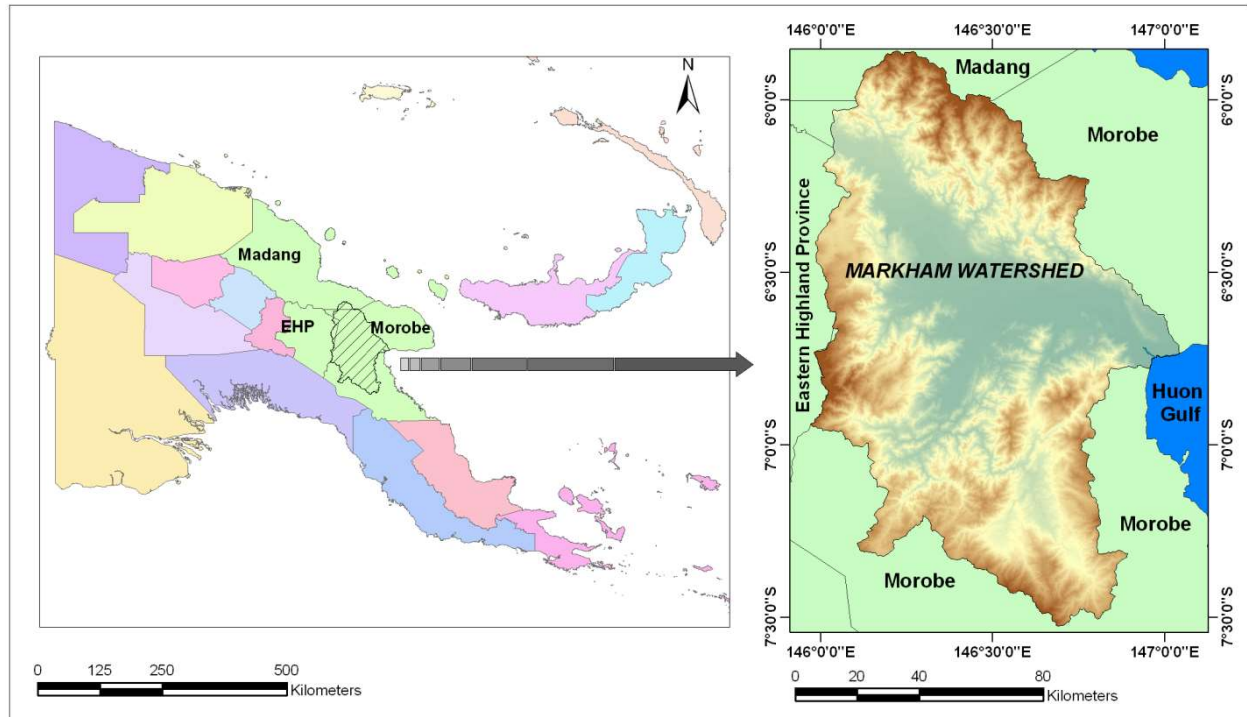


Fig. 1 Location map of the Markham watershed area

In order to calculate the TWI, a series of analysis were performed with the help of spatial analysis toolbox within ArcMap, namely fill DEM, flow direction, flow accumulation, slope in degree, radian slope, tan slope and scaled flow accumulation (Kopecký et al., 2021). Figure 2 briefly represents the methodology of TWI database generation. The geo-processing Fill tool (spatial analysis) of ArcGIS was used to fill the sinks of the ASTER DEM data. This process removes the small-scale imperfections in any raster elevation data sets (Zhou et al., 2022). Flow direction establishes the direction of water flow from one cell to another based on the steepest descents in each cell (Reed, 2003). Flow accumulation represents number of cell or the upstream area that draining into each cell (Arnold, 2010). Flow direction was calculated using “Flow Direction” algorithm within Hydrology section of the Spatial Analyst tools under Arc Toolbox in ArcGIS using filled DEM data. The output flow direction was used as input to calculate the flow accumulation using “Flow Accumulation” algorithm. Slope in degree, radian slope, tan slope and scaled flow accumulation were calculated through equation 2 to 5 respectively using “raster calculator” under Map Algebra of the Spatial Analyst tools.

$$\text{Slope in Degree} = \arctan(\text{rise/run}) \quad (\text{eq. 2})$$

$$\text{Radians of Slope} = \frac{\text{Slope in degree} * 1.570796}{\text{cell size}} \quad (\text{eq. 3})$$

$$\text{Tan Slope} = \text{Con}(\text{Slope} > 0, \tan(\text{slope}), 0.001) \quad (\text{eq. 4})$$

$$\text{Flow Accumulation Scaled} = (\text{Flow Accumulation} + 1) * \text{Cell Size} \quad (\text{eq. 5})$$

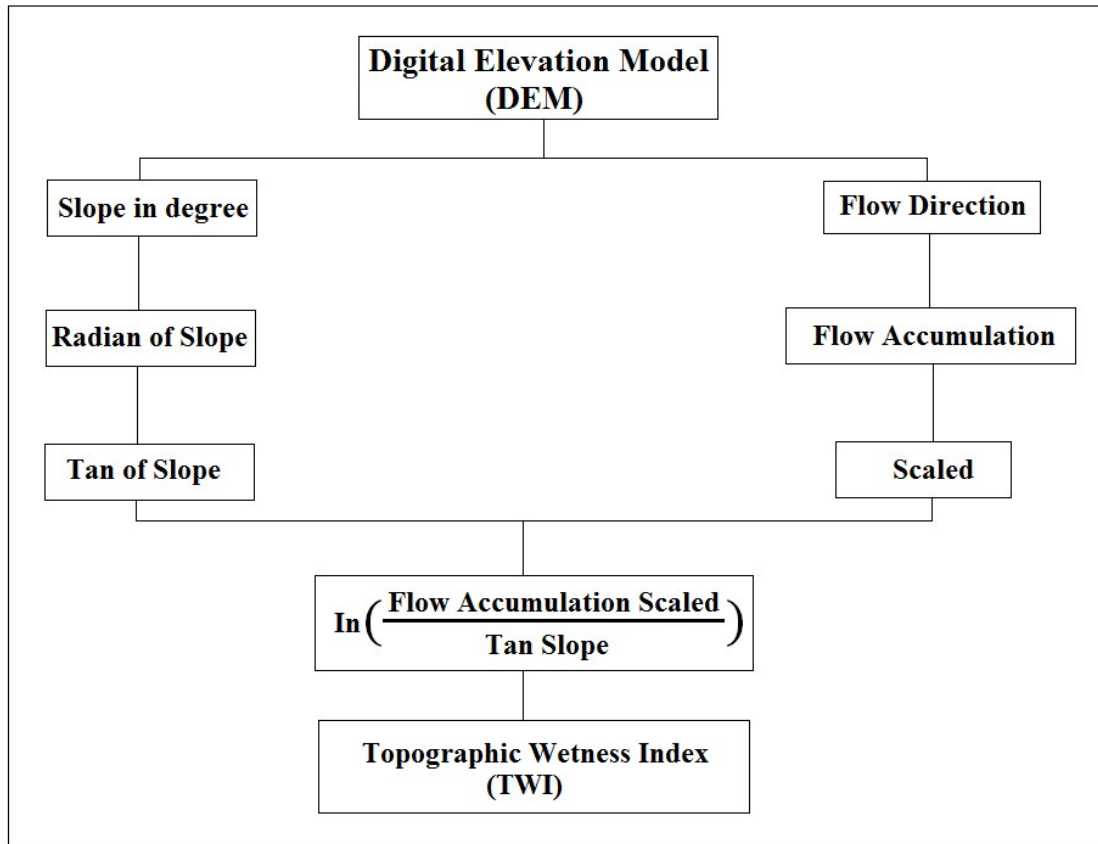


Fig. 2 The methodological flow chart for the preparation of Topographic Wetness Index map

3. Results and Discussion

The maximum altitude 4096.45 m is found in the north part of the watershed, from where the Markham river originated (Figure 3a). The Markham watershed is characterised by high up and down slope (Samanta and Bhunia, 2013). The highest slope is observed as 89.09 degree at some pockets of the watershed as presented with red colour (Figure 2b). Very low altitude and very gentle slope is identified at the middle portion of the watershed, where the Markham valley is situated. The spatial distribution of radian slope and the tan slope is almost similar with different output value. Maximum radian of slope was calculated as 1.55 with an average value of 0.31 and the highest tan slope of 63.18 was observed along with the mean value of 0.34 respectively in the Markham watershed area (Figure 3c and 3d). The output of the flow direction represents the direction of the flow of each cell in the raster surface, which range from 1 to 128. These values are representing different directions on the map. For example, value 1 represent East, 2 for North-East, 4 for South, 8 for South-West, 16 for West, 32 for North-West, 64 for North and 128 for North-East respectively (Figure 3e). The calculated average flow accumulation was classified into 5 categories to show its spatial distribution (Figure 3f).

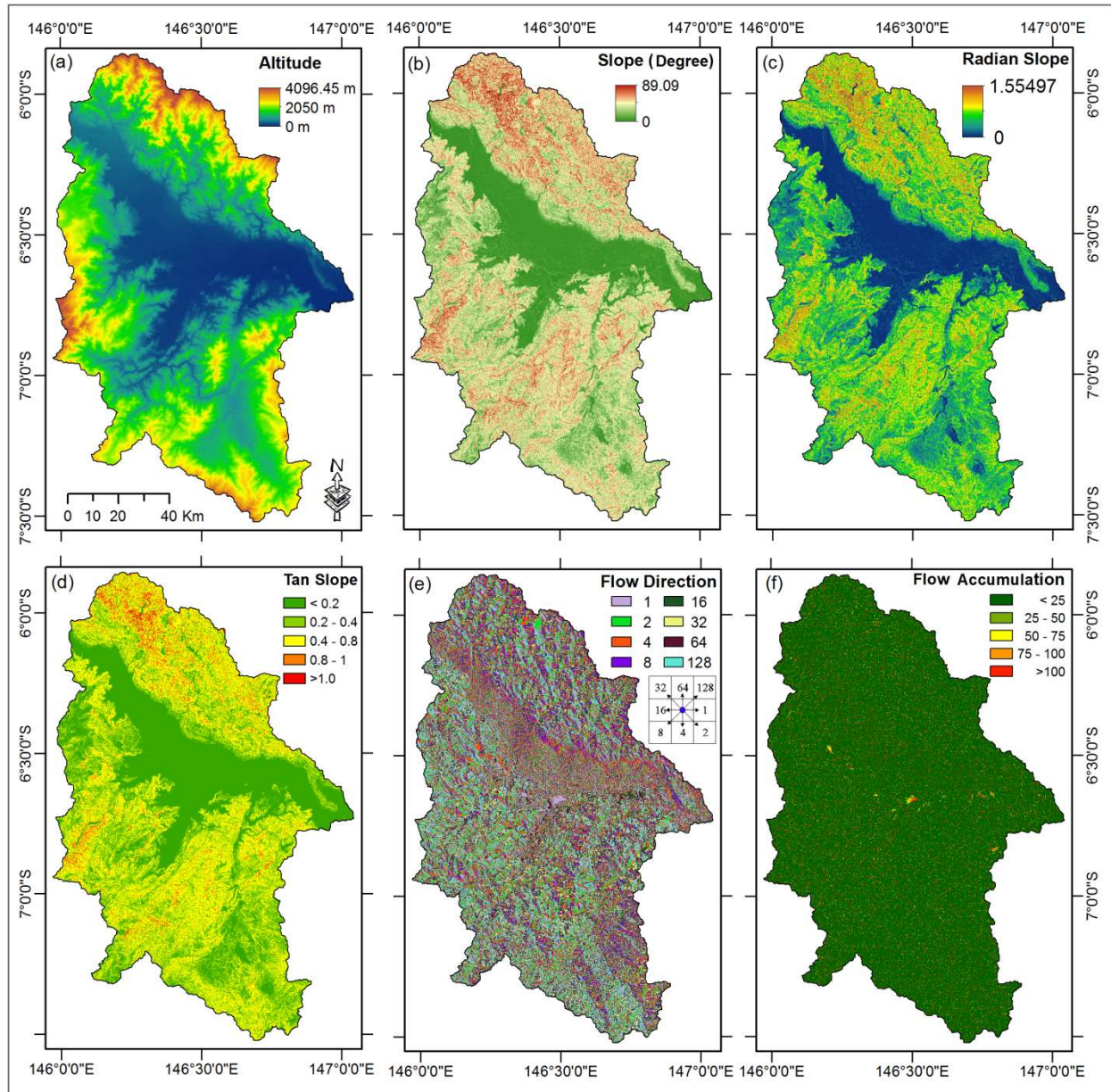


Fig. 3 Topographic parameters to calculate TWI (a) Digital Elevation Model, (b) Slope in degree, (c) Radian Slope, (d) Tan Slope, (e) Flow Direction and (f) Flow Accumulation.

The final topographic wetness index (TWI) was calculated using a normalised equation (Equation 6) which is similar to the equation 1.

$$TWI = \ln\left(\frac{\text{Flow Accumulation Scaled}}{\text{Tan Slope}}\right) \quad (\text{eq. 6})$$

The output TWI is ranged from 0.6 to 42.3 (Figure 4a) with an average value of 6.81 (Figure 4a). The TWI database was further reclassified into 5 categories (Figure 4b), which are essential sub categories for hydrological modeling (Table 1).

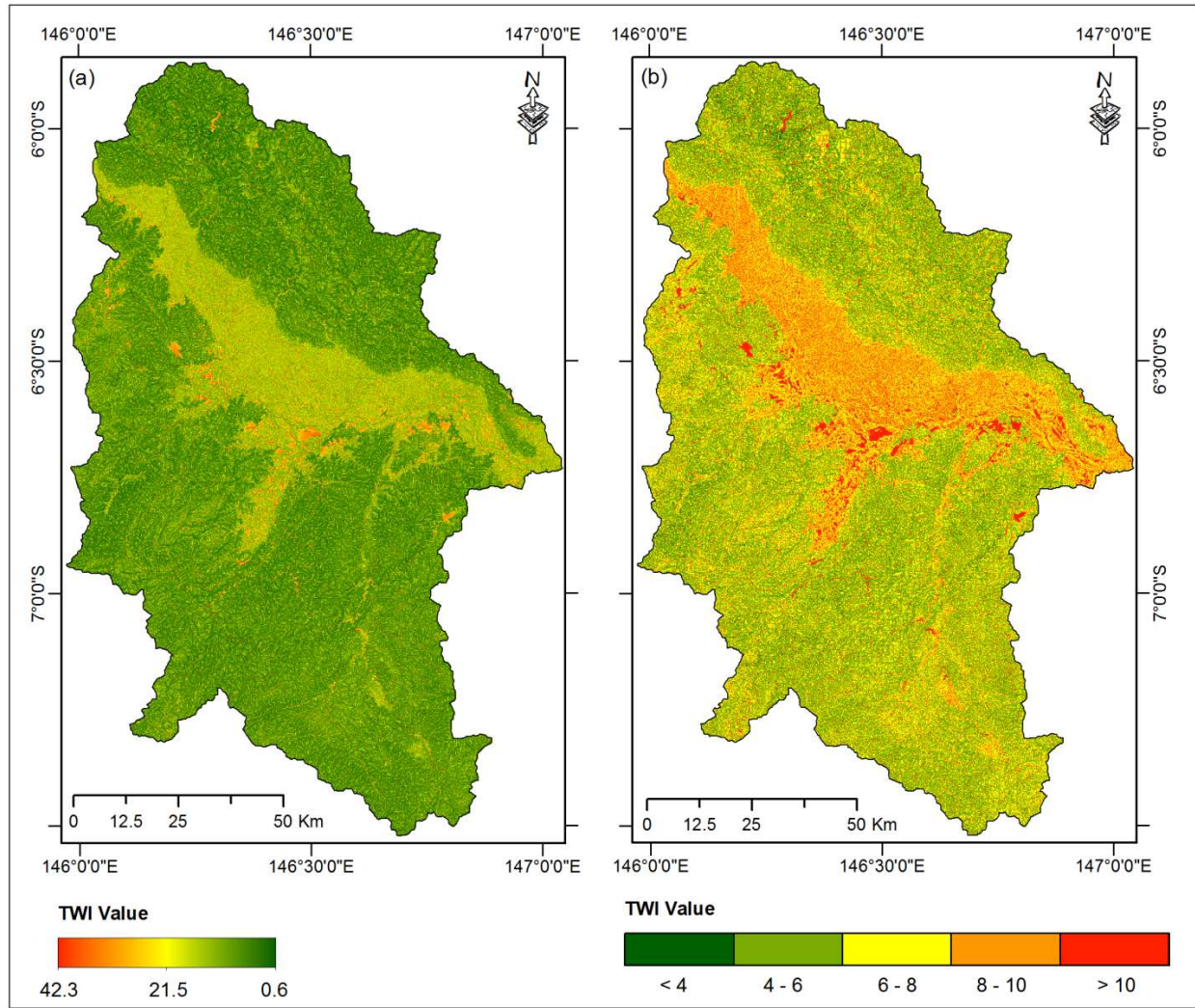


Fig. 4 Topographic Wetness Index map represented with (a) Stretched TWI value and (b) classified (5 classes) TWI value

Table 1. Classified topographic wetness index (TWI)

TWI range	Average TWI	Classified TWI		Area in hectare	% of area
		TWI range	TWI impact class to soil moisture		
0.6 (low) to 42.6 (high)	6.81	Less than 4	Very low	24242.22	1.9
		4 – 6	Low	554938.1	43.5
		6 – 8	Medium	444637.9	34.8
		8 – 10	High	142286.7	11.1
		More than 10	Very High	110485.6	8.7

Lower TWI value has less impact and higher value impact significantly to the soil moisture and the plant growth in an agriculture or plantation region. The very high TWI is found in the middle part of the watershed area where the topographic slope is very gentle. The very low TWI classes are observed in the higher topographic slope area. The spatial distribution of TWI is a dependent factor of the topographic slope (Sörensen et al., 2006; Besnard et al., 2013).

A linear regression analysis was performed to understand the relationship between TWI and Slope of the Markham watershed. The Geo-processing tool, 'Create fishnet' under data management of Arc Toolbox of ArcGIS v10.5 (ArcMap) was used to create fishnet points (Samanta et al., 2018; Pan et al., 2022) around the study area. Five thousand (5000) fishnet points were generated in a rectangle dimension (50 points x 100 points). Afterward, the points that fall within the Markham watershed area were extracted through the intersection process between the fishnet point layer and the watershed boundary layer. The cell values of TWI and the slope were extracted at each fishnet point location using 'Extract multi values to point' tool under spatial analyst of ArcMap. The linear regression equation and R-square value was calculated in the Microsoft Excel. The value of R-square refers to the coefficient of determination and the value ranged between 0 and 1 or 0% to 100%. R-squared Value of less than 0.3 means weak relationship, while value between 0.3 and 0.5 is moderate and value more than 0.7 means strong relationship between the variable (Srinivasan, 2020). The strength of the relationship or R-squared value between Slope (linear model) and the TWI (dependent variable) was calculated as 0.38, which is moderately correlated (Figure-5).

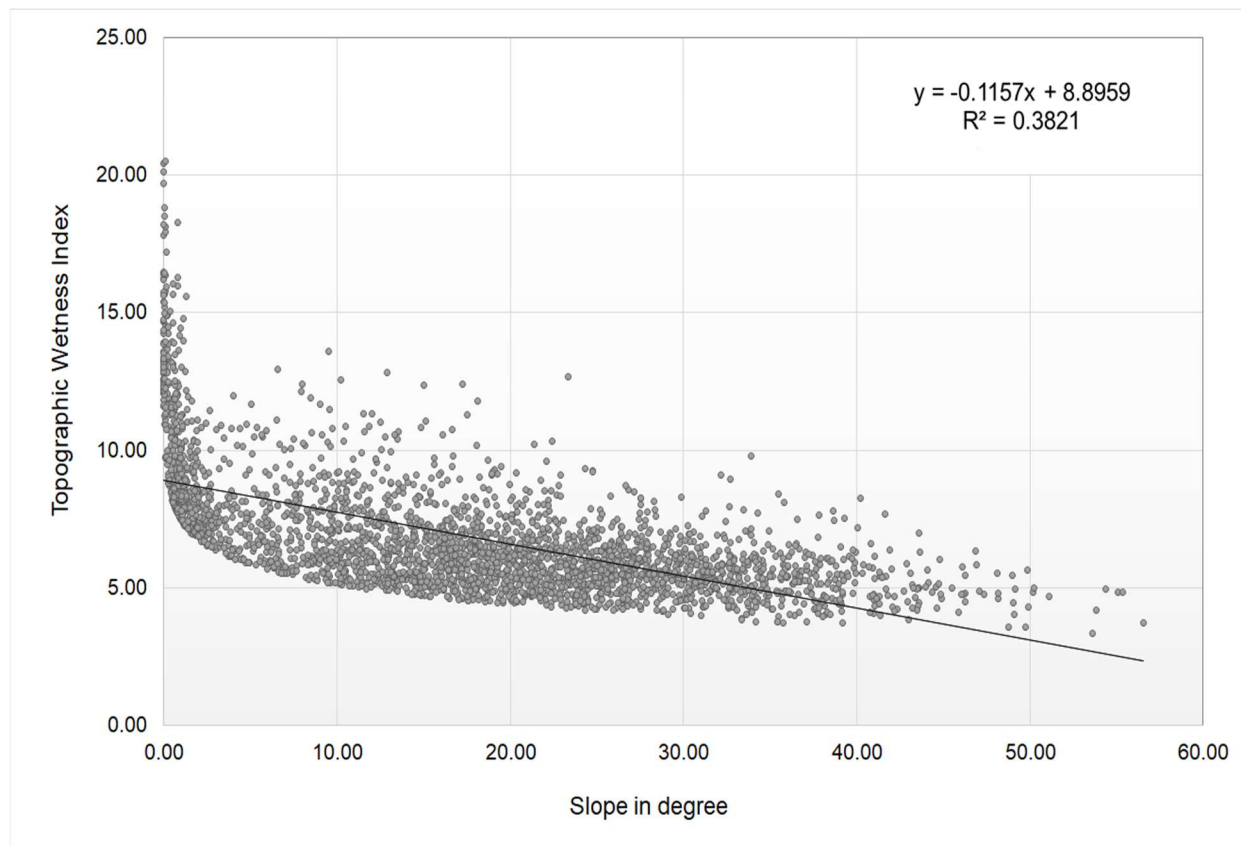


Fig. 5 The R square value in the linear regression model between Slope and TWI

4. Conclusion and recommendations

In this paper, the detailed methodology of topographic wetness index (TWI) preparation was established using the advanced space borne thermal emission and reflection radiometer (ASTER) derived DEM data and ArcGIS v10.5 software. The variation of the spatial resolutions of the topographic data (i.e. DEM) may yield different results for the same watershed area (Chowdhury, 2023). So, the resolution factor of a topographic data (DEM) has to be defined in research. A spatial resolution of 30m DEM data was used in this present study. The study produces void-less wall-to-wall topographic wetness index data for the Markham watershed area. The study also rebuild that the topographic slope has the largest influence on the topographic wetness index. In the absence of the soil moisture data TWI can be an alternative option to be used as a proxy for soil moisture (Riihimäki et al., 2021). The TWI can be used to evaluate species richness, soil pH, groundwater level, surface water storage sites, landslide probability, hydrological modelling for flood early warning, identifying potential soil erosion risk areas or any other hydrological analysis in any watershed area with the help of other associated parameters.

5. References

1. Abrams, M. (2000). The Advanced Spaceborne Thermal Emission and Reflection Radiometer (ASTER): data products for the high spatial resolution imager on NASA's Terra platform. *International Journal of Remote sensing*, 21(5), 847-859. <https://doi.org/10.1080/014311600210326>
2. Abrams, M., Tsu, H., Hulley, G., Iwao, K., Pieri, D., Cudahy, T., and Kargel, J. (2015). The advanced spaceborne thermal emission and reflection radiometer (ASTER) after fifteen years: review of global products. *International Journal of Applied Earth Observation and Geoinformation*, 38, 292-301. <https://doi.org/10.1016/j.jag.2015.01.013>
3. Arnold, N. (2010). A new approach for dealing with depressions in digital elevation models when calculating flow accumulation values. *Progress in Physical Geography*, 34(6), 781-809. <https://doi.org/10.1177/0309133310384542>
4. Besnard, A. G., La Jeunesse, I., Pays, O., and Secondi, J. (2013). Topographic wetness index predicts the occurrence of bird species in floodplains. *Diversity and Distributions*, 19(8), 955-963. <https://doi.org/10.1111/ddi.12047>
5. Beven, K. J. and Kirkby, M. J. (1979). A physically based, variable contributing area model of basin hydrology, *Hydrological sciences journal*, 24, 43-69. <https://doi.org/10.1080/02626667909491834>
6. Brookfield, A. E., Ajami, H., Carroll, R. W. H., Tague, N., Sullivan, P. L., and Condon, L. (2023). Recent advances in integrated hydrologic models: Integration of new domains. *Journal of Hydrology*, 620(B), 129515. <https://doi.org/10.1016/j.jhydrol.2023.129515>
7. Buchanan, B. P., Fleming, M., Schneider, R. L., Richards, B. K., Archibald, J., Qiu, Z., and Walter, M. T. (2014). Evaluating topographic wetness indices across central New York agricultural landscapes. *Hydrology and Earth System Sciences*, 18(8), 3279-3299. <https://doi.org/10.5194/hess-18-3279-2014>.

8. Chowdhury, M. S. (2023). Modelling hydrological factors from DEM using GIS. *MethodsX*, 10, 102062. <https://doi.org/10.1016/j.mex.2023.102062>.
9. Das, S. (2018). Geographic information system and AHP-based flood hazard zonation of Vaitarna basin, Maharashtra, India. *Arabian Journal of Geosciences*, 11(19), 576. <https://doi.org/10.1007/s12517-018-3933-4>
10. Easton, Z. M., Fuka, D. R., Walter, M. T., Cowan, D. M., Schneiderman, E. M., and Steenhuis, T. S. (2008). Re-conceptualizing the soil and water assessment tool (SWAT) model to predict runoff from variable source areas. *Journal of hydrology*, 348(3-4), 279-291. <https://doi.org/10.1016/j.jhydrol.2007.10.008>
11. Grabs, T., Seibert, J., Bishop, K., and Laudon, H. (2009). Modeling spatial patterns of saturated areas: A comparison of the topographic wetness index and a dynamic distributed model. *Journal of Hydrology*, 373(1-2), 15-23. <https://doi.org/10.1016/j.jhydrol.2009.03.031>
12. Hojati, M., & Mokarram, M. (2016). Determination of a topographic wetness index using high resolution digital elevation models. *European Journal of Geography*, 7(4), 41-52.
13. Hu, Z., Peng, J., Hou, Y., and Shan, J. (2017). Evaluation of recently released open global digital elevation models of Hubei, China. *Remote Sensing*, 9(3), 262.
14. Kopecký, M., Macek, M., and Wild, J. (2021). Topographic Wetness Index calculation guidelines based on measured soil moisture and plant species composition. *Science of the Total Environment*, 757, 143785. <https://doi.org/10.1016/j.scitotenv.2020.143785>
15. Koriche, S. A., and Rientjes, T. H. (2016). Application of satellite products and hydrological modelling for flood early warning. *Physics and Chemistry of the Earth, Parts A/B/C*, 93, 12-23. <https://doi.org/10.1016/j.pce.2016.03.007>
16. Pan, J., Wu, X., Zhou, L., and Wei, S. (2022). Spatial and temporal distribution characteristics of active fires in china using remotely sensed data. *Fire*, 5(6), 200. <https://doi.org/10.3390/fire5060200>
17. Pournali, S. H., Arrowsmith, C., Chrisman, N., Matkan, A. A., and Mitchell, D. (2016). Topography wetness index application in flood-risk-based land use planning. *Applied Spatial Analysis and Policy*, 9, 39-54. <https://doi.org/10.1007/s12061-014-9130-2>
18. Reaney, S. M., Lane, S. N., Heathwaite, A. L., and Dugdale, L. J., (2011). Risk-based modelling of diffuse land use impacts from rural landscapes upon salmonid fry abundance, *Ecological Modelling*, 222(4), 1016–1029. <https://doi.org/10.1016/j.ecolmodel.2010.08.022>.
19. Reed, S. M. (2003). Deriving flow directions for coarse-resolution (1–4 km) gridded hydrologic modeling. *Water resources research*, 39(9). <https://doi.org/10.1029/2003WR001989>
20. Riihimäki, H., Kemppinen, J., Kopecký, M., and Luoto, M. (2021). Topographic wetness index as a proxy for soil moisture: The importance of flow-routing algorithm and grid resolution. *Water Resources Research*, 57(10), e2021WR029871. <https://doi.org/10.1029/2021WR029871>
21. Samanta, S., and Bhunia, G. S. (2013). Landslide susceptibility zone identification of Markham Watershed, PNG A study based on remote sensing and GIS technology. *International Journal of Physical and Social Sciences*, 3(1), 307-322.
22. Samanta, S., Pal, D. K., and Palsamanta, B. (2018). Flood susceptibility analysis through remote sensing, GIS and frequency ratio model. *Applied Water Science*, 8(2), 66. <https://doi.org/10.1007/s13201-018-0710-1>
23. Schneiderman, E. M., Steenhuis, T. S., Thongs, D. J., Easton, Z. M., Zion, M. S., Neal, A. L., Mendoza, G.F., and Walter, M.T. (2007). Incorporating variable source area hydrology

- into a curve number-based watershed model. *Hydrological Processes*, 21(25), 3420-3430. <https://doi.org/10.1002/hyp.6556>
24. Sorensen, R., Zinko, U. and Seibert, J., (2006). On the calculation of the topographic wetness index: evaluation of different methods based on field observations. *Hydrology and Earth System Sciences*, 10(1), 101-112. <https://doi.org/10.5194/hess-10-101-2006>.
25. Srinivasan, P. (2020). Interpreting p-value and R squared score on real-time data—statistical data exploration. *Data Science Blogathon*, 2-3.
26. Suzen M.L., and Kaya B. S. (2012). Evaluation of environmental parameters in logistic regression models for landslide susceptibility mapping. *International Journal of Digital Earth*, 5(4), 338–355. <https://doi.org/10.1080/17538947.2011.586443>
27. Wang, L., and Liu, H. (2006). An efficient method for identifying and filling surface depressions in digital elevation models for hydrologic analysis and modelling. *International Journal of Geographical Information Science*, 20(2), 193-213.
28. Yang, L., Meng, X., and Zhang, X. (2011). SRTM DEM and its application advances. *International Journal of Remote Sensing*, 32(14), 3875-3896. <https://doi.org/10.1080/01431161003786016>
29. Zhou, G., Song, B., Liang, P., Xu, J., and Yue, T. (2022). Voids filling of DEM with multiattention generative adversarial network model. *Remote Sensing*, 14(5), 1206. <https://doi.org/10.3390/rs14051206>

Author's Bibliography

Dr. Sailesh Samanta is presently working as Associate Professor and GIS Section Head in the Department of Surveying and Land Studies at The Papua New Guinea University of Technology, Papua New Guinea. His research profile can be accessed through <https://scholar.google.com/citations?user=vd3ddccAAAAJ>